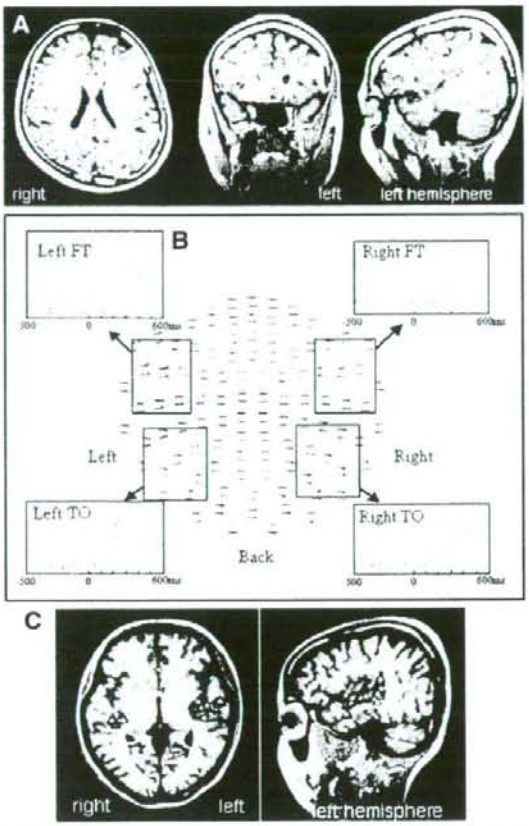

FIGURE 1. *A 24-year-old, right-handed man with epilepsy.* A, *fMRI with the verb generation task showing activations predominantly in the left IFG, MFG, PrecG, and parieto-occipital regions.* B, *square root mean field profiles of language MEG responses in the bilateral FT and TO regions. The left FT responses, peaking at 450 milliseconds, were markedly greater in amplitude than the right FT.* C, *source localization of the late deflections showing predominant dipole clusters (arrowheads) in the left superior temporal region. The left and right hemispheres contained 97 and 37 dipoles, respectively.*

ral region (FuG and inferior temporal gyrus). In 96 patients who showed unilateral language dominance, the total number of dipoles in the dominant versus non-dominant hemispheres was 124.1 ± 62.1 and 58 ± 30.9 (mean ± standard deviation), respectively. The ratio of the dipole number in the dominant hemisphere to the non-dominant hemisphere in each individual was 2.4 ± 1.7 (range, 1.43–14.4).

A typical result with all channels of MEG with the *Kana*-reading task is illustrated in *Figure 1*. Later deflections peaking at approximately 400 milliseconds were predominantly observed in the left FT. Bilateral TO regions demonstrated early deflections at approximately 200 milliseconds with short durations and little laterality. Estimated dipoles of the FT regions were densely accumulated in the left STG, MTG, and SmG (102 dipoles), whereas the right hemisphere showed fewer dipoles (54 dipoles) in the superior temporal region. This patient was thus determined to have receptive language dominance in the left temporal lobe.

The successful rate of language-MEG was 82.4%. Nine out of 39 epilepsy patients (23.1%) could not provide useful MEG data owing to artifacts from constant eye movements; the *Kana*-reading task was more difficult to complete than the verb generation task for patients with mental dysfunction. On the other hand, only one out of 18 AVM patients, owing to severe dyslexia, failed to provide useful MEG data, indicating that, in contrast to fMRI, MEG was not frequently affected by cerebral blood flow abnormalities (*Fig. 3*).

Combination of fMRI and MEG with Wada Test Verification

The verb generation task fMRI data depict expressive language areas well, but may be affected by cerebral blood flow abnormalities. The MEG results indicate receptive language areas well, but the task is rather complicated and may not be suited for patients with mental disorders. We sought to establish a non-invasive and reliable method to determine the laterality of language dominance by combining the advantages of these approaches. Furthermore, in terms of language functions, the results from fMRI and MEG can be integrated to locate expressive and receptive language areas and to provide reliable evidence whether or not there is dissociation. To verify the reliability of our method, 97 patients also underwent the Wada test.

Useful data from the method co-utilizing fMRI and MEG could be obtained from 87 out of 91 patients (95.6%). Remarkably, regarding language dominance, the results from the combination method matched the results of the Wada test in all 87 patients. Worth noting is that two patients (one with left temporal lobe epilepsy and the other with right insular astrocytoma) showed dissociated language areas using the combined method. The expressive language area was depicted in the left frontal lobe by fMRI, but the receptive language area was demonstrated in the right temporal lobe by MEG (*Fig. 4*). The Wada test results confirmed that both patients have language functions dissociated in the bilateral hemispheres. Among the 91 patients who underwent the Wada test, these were the only two patients in whom the Wada test detected dissociation of language functions.

In 12 epilepsy patients, the expressive and/or receptive language areas were electrophysiologically investigated via a subdural electrode implantation and the results were compared with those determined via the combined fMRI plus MEG method (*Fig. 5*). Out of eight patients who underwent cortical mapping for the expressive language area, all showed a speech arrest by electrical stimulation to the IFG and four to the MFG. All of the physiologically determined locations were confined within the areas depicted by the combined method. Out of six patients who received electrical stimuli to the temporal lobe,

four showed responses interpretable as impaired speech comprehension. In all such cases, the electrophysiologically determined location matched the area depicted by the combined method, although MEG-depicted receptive language areas covered relatively broad areas of the temporal lobe. The regions determined by the combined method were always broader, but had the border within the adjacent gyri of those determined by electrophysiological mapping.

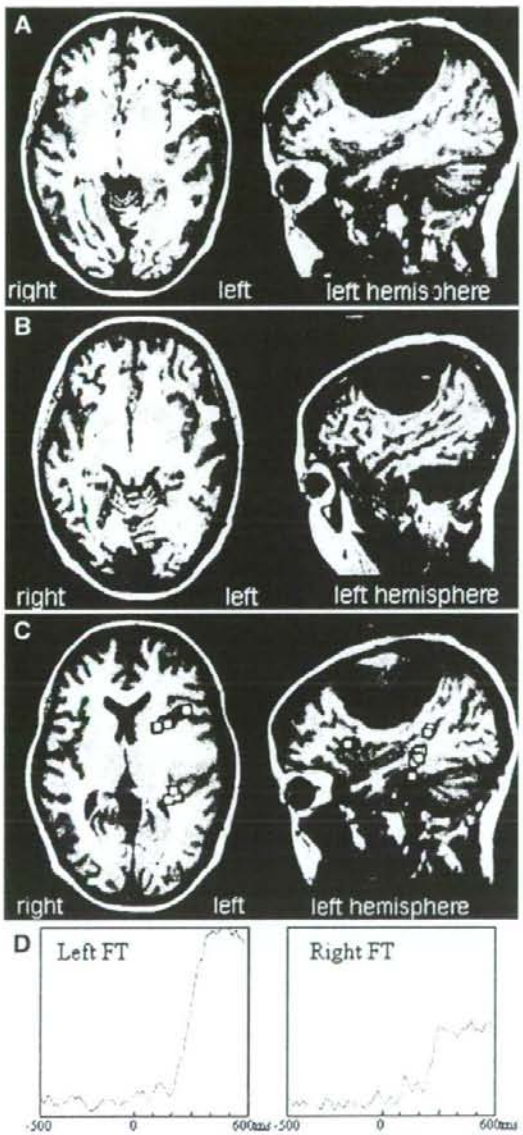

FIGURE 2. *A 16-year-old, right-handed female patient with a large meningioma in the left frontal region. The patient had no impairment of language or motor functions. A, fMRI with the verb generation task showed activations mainly in the left IFG and MFG that shifted inferiorly by the tumor. B, fMRI with the abstract/concrete categorization task demonstrated activations in the bilateral occipital regions in addition to small active spots in the left IFG. C, square root mean field profiles of language-MEG responses demonstrated that the left FT responses, peaking at 400 milliseconds, were markedly larger in amplitude than the right FT. D, source localization of the late deflections showed predominant dipole clusters in the left posterior temporal region. The left and right hemispheres contained 117 and 30 dipoles, respectively. The combined fMRI plus MEG method indicated left language dominance, which was confirmed by Wada test.*

ILLUSTRATIVE CASES

Patient 1

A 16-year-old, right-handed female patient had experienced transient numbness in her left upper extremity with a 2-month history. T1-weighted MRI scans demonstrated an extra-axial cystic lesion in the left frontal region. Although the lesion markedly compressed the frontal lobe, she had no impairment of language and motor functions. fMRI with the verb generation task demonstrated obvious activation in the left IFG and MFG shifted inferiorly by the lesion (*Fig. 2A*). The A/C categorization task activated a small area of the left IFG, but mainly the bilateral occipital lobes. Concerning MEG with the *Kana* reading task, RMS of the left FT was much higher than that of the right, and numbers of semantic dipoles were 117 and 30 in left and right hemispheres, respectively. The main dipole clusters were located in the left IFG and STG. The tumor was totally removed and histopathological diagnosis was meningioma.

Patient 2

A 24-year-old, right-handed male patient had a large AVM in the left frontal lobe. fMRI detected little activation in the IFG or MFG, although a part of the left angular gyrus was activated by the verb generation task (*Fig. 3A*). MEG, however, disclosed numerous dipole accumulations in the left superior temporal region. In the MEG examination, the left and right hemispheres contained 130 and 45 dipoles, respectively, suggesting left language dominance (*Fig. 3B*). Auditory comprehension and letter-reading were suppressed by administration of amobarbital into the left carotid artery, although motor language function was preserved. These findings suggested that the steal effect caused by the AVM partly interfered with functional brain mapping of fMRI and the Wada test. In this case, MEG was helpful to decide language dominance (*Fig. 3*).

Patient 3

A 32-year-old, right-handed man experienced amnesia for several minutes. T1-weighted MRI scans and brain computed tomographic scans disclosed a hypointense and hypodense mass in the right insular cortex involving the surrounding white matter. Computed tomographic scans performed 6 years earlier, however, revealed no abnormality. These findings suggested that a low-grade astrocytoma might

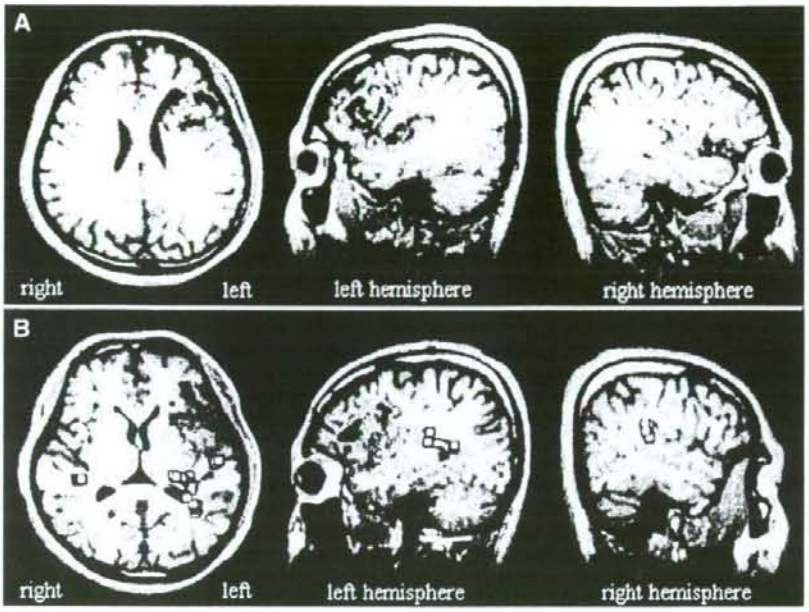

FIGURE 3. *A 24-year-old, right-handed man with a large AVM in the left frontal lobe. A, fMRI with the verb generation task showed little activation in the left frontal lobe where the AVM was located. B, source localization of the late FT and TO deflections on MEG showed predominant dipole clusters in the left posterior STG. The left and right hemispheres contained 123 and 51 dipoles, respectively.*

have slowly developed during the past 6 years. In the results of the verb generation task, the left hemisphere had obvious activations in the IFG, MFG, precG, and the angular gyrus, indicating that this patient had left dominance of motor-language functions (*Fig. 4A*). In contrast, estimated dipoles of the FT responses were concentrated in the posterior part of the right STG and MTG (138 dipoles) and another dipole cluster (64 dipoles) of the TO region was localized in the right FuG. The total dipole number of the left hemisphere (48 dipoles) did not reach even a quarter of that of the right hemisphere, suggesting right-sided dominance of temporal language functions (*Fig. 4*).

During the Wada test, he stopped counting (0 out of 4 points; 0%) and failed to name objects (6 out of 20 points; 30%) after left intracarotid injection, whereas letter-reading (21 out of 28 points; 75%), auditory comprehension (12 out of 12 points, 100%), and pointing objects tasks (16 out of 16 points; 100%) were well preserved. In contrast, after right intracarotid injection, letter reading (13 out of 28 points; 45%), auditory comprehension (3 out of 12 point; 25%), and pointing objects (4 out of 16 points; 25%) tasks were markedly suppressed, although he continued to count correctly without speech blockade (4 out of 4 points; 100%) and could perform naming (17 out of 20 points; 85%). These findings suggested that language functions were distributed separately over the bilateral hemispheres, and the expressive and receptive language functions were dissociated in the left frontal and right temporal lobes, respectively. A striking fact was that the combination of fMRI and MEG predicted the special profiles of language functions noninvasively.

DISCUSSION

We demonstrated that our method using both fMRI with the verb generation task and MEG with the *Kana* reading task is highly reliable in determining the language dominance in patients with brain lesions. The accuracy of the dominance laterality was confirmed by a 100% match with the results from the Wada test. fMRI and MEG compensated each other's disadvantages. The tasks of fMRI were rather simple and could be accomplished even by patients with mental dysfunctions, whereas MEG results were seldom affected by cerebral blood flow abnormalities. Reliable data on language functions were also obtained by combining the advantageous features of fMRI and MEG. fMRI with the verb generation task well depicted the expressive language area as activations in the frontal lobe, most commonly in the IFG. MEG, on the other hand, showed dipole clusters predominantly in the superior temporal regions representing the receptive language area. In the epilepsy group, left and bilateral dominance were approximately 85% and more than 6%, respectively, whereas, in the non-epilepsy group, left and bilateral dominance were more than 90% and less than 2%, respectively. The combined method, including the Wada test, fMRI, and MEG, clearly demonstrated bilateral dominance is more often observed in the epilepsy group than in the non-epilepsy group.

In our study, two out of 87 patients analyzed (2.3%) were found to have dissociation of the expressive and receptive language functions by co-utilization of fMRI and MEG, verified by the Wada test, which best described the usefulness of our method in identifying the areas of the two language functions separately. In both cases, neither modality alone demonstrated the dissociation. Although several cases have been reported that dissociated language functions were found by fMRI, none of those was proven by the Wada test (2, 8, 21, 23). Our results show that neither fMRI nor MEG alone is sufficient to accurately locate the expressive and receptive language areas, and the combined use is the key to obtaining high reliability.

The results from electrophysiological investigation via a subdural electrode implantation in 12 patients further confirmed the accuracy of the present method. Pouratian et al. (22) reported that the sensitivity and specificity of language-fMRI

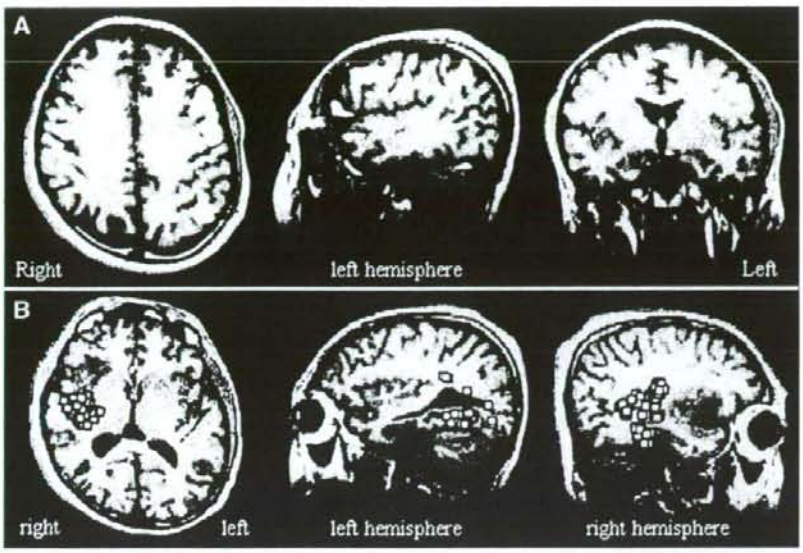

FIGURE 4. *A 32-year-old, right-handed man with astrocytoma in the right insular cortex and the surrounding white matter. A, fMRI with the verb generation task showed main activations in the IFG, MFG, precG, and AG, indicating left dominance of the expressive language function. B, in contrast to the fMRI results, source localization of the late FT deflections on MEG showed predominant dipole clusters in the right temporal lobe. The left and right hemispheres contained 48 and 202 dipoles, respectively. The combined fMRI plus MEG method thus indicated dissociated frontal motor and temporal receptive language functions. This result was confirmed by the Wada test. The patient showed impaired counting and object naming after amobarbitol injection into the left carotid artery. In contrast, letter reading, auditory comprehension and object pointing tasks were markedly suppressed, without counting impairment and speech blockade, after amobarbitol injection into the right carotid artery.*

were dependent on the task, lobe, and matching criterion. The sensitivity and specificity of fMRI activations during expressive linguistic tasks in the frontal lobe were found to be up to 100 and 66.7%, respectively, in the frontal lobe. FitzGerald et al. (6) reported that sensitivity and specificity for all multiple language tasks ranged from 81 to 53% (6). On the other hand, several groups have reported that the language map obtained from fMRI poorly matched the intraoperative electrical stimulation mapping (6, 25). In our study of language-fMRI, every electrical stimuli to the IFG, where the fMRI-activation was observed, caused speech arrest. However, the stimulation to MFG caused language-related symptoms in only half of patients. Although the sensitivity of fMRI might be high, there are still several issues of individual variability of fMRI activation and semantic tasks. The discrepancy can be partly accounted for by the fundamental differences in methodology such that the electrical stimulation directly blocks the specific language functions, whereas fMRI picks up all activated areas involved in the language tasks. Therefore, fMRI-based mapping largely depends on the design of the performing task. We tested two different tasks for fMRI and found the verb generation task better suited for language mapping than the A/C categorization task. The significance of activations depicted on fMRI is still under debate. Language-fMRI activations may be related to various semantic components of the task, including the will to retrieve verbal materials and the memory related to articulations. Despite that the A/C categorization task was designed to detect the receptive language area, activations in the temporoparietal region was less frequently observed than in the frontal region. Neural activities in the temporoparietal area are considered relatively scarce (25), and the discrepant activities of the frontal and temporoparietal regions may be owing to physiological variations of brain regions. Alternatively, the frontal and temporal lobes may have different oscillations (brain rhythms) of brain activity in response to verbal tasks, which are reflected in changes in neuronal currents and cerebral blood flow.

Our study demonstrated that dominance of the receptive language function could be accurately determined by MEG. For that purpose, we originally designed the task of three-letter word reading and silent categorization and used the dipoles calculated from late deflections to process the MEG results. It has been reported that cortical evoked potentials recorded by subdural electrodes showed responses at approximately 200 (early) and 400 (late) milliseconds in the left temporal lobe cortex after letter presentation (1, 17). The late potentials have been noted especially in tasks involving decisions based on visually presented words (13, 14). In this study, the sources of late responses (250–600 ms) were located mostly in the posterior temporal region, and the laterality of dipole clusters accurately reflected the receptive language dominance. It has been reported that dipoles in the superior temporal region showed an excellent agreement with an intraoperative electrical mapping (27). We also included dipoles in the FuG for language dominance determination based on our experience with a case in which an injury of FuG resulted in pure dyslexia (12). These contrivances in our method may have led to improvement in accuracy on language dominance determination over previous reports (20). Basic technical issues of the MEG investigation still remain. Eye movement artifacts were strong enough to distort the baseline of the MEG data. In our study,

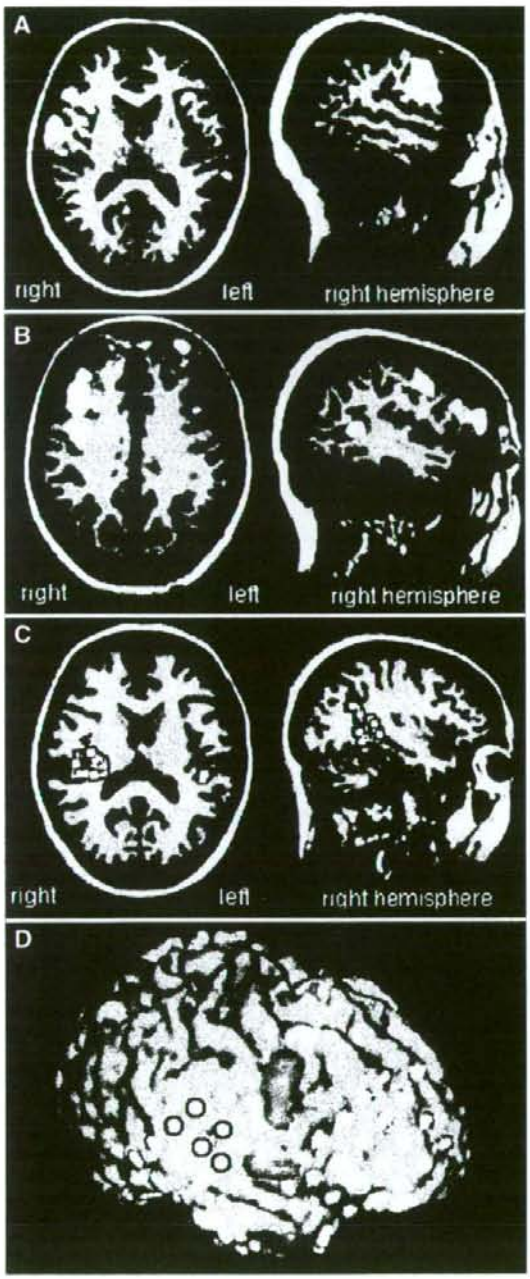

we asked patients to keep gazing at the center of the screen during the semantic decision without blinking. As a result, artifacts were observed at later than 600 milliseconds after letter presentation and usually did not affect the early and late semantic responses. It is, however, important to prevent artifacts by monitoring eye movements and using rejection thresholds.

In conclusion, by co-utilizing fMRI and MEG, we established a method to determine language dominance with a high reliability. The fMRI activations with the verb generation task identified the expressive language area, whereas the language MEG dipoles located the receptive language areas. Our institution is now routinely using the combined technique to identify the language dominance. If it does not produce data on cerebral dominance, we additionally perform the Wada test before surgery. This non-invasive and repeatable method may be an effective alternative to the Wada test and may be useful in the management of patients with brain lesions.

Disclosure

This work was supported in part by the Japan Epilepsy Research Foundation, Takeda Promotion of Science Foundation, a grant-in-aid No.17591502 for scientific research from MEXT, a Research Grant of the Princess Takamatsu Cancer Research Fund, Terumo Promotion of Science Foundation, Brain Science foundation, and Grant-in-Aid No. 18020010 for Scientific Research on Priority Areas Integrative Brain Research from MEXT.

REFERENCES

1. Allison T, McCarthy G, Nobre A, Puce A, Belger A: Human extrastriate visual cortex and the perception of faces, words, numbers, and colors. **Cereb Cortex** 4:544–554, 1994.
2. Baciu MV, Watson JM, McDermott KB, Wetzel RD, Attarian H, Moran CJ, Ojemann JG: Functional MRI reveals an interhemispheric dissociation of frontal and temporal language regions in a patient with focal epilepsy. **Epilepsy Behav** 4:776–780, 2003.
3. Branch C, Milner B, Rasmussen T: Intracarotid sodium amytal for the lateralization of cerebral speech dominance: Observations in 123 patients. **J Neurosurg** 21:399–405, 1964.
4. Brazdil M, Zakopcan J, Kuba R, Fanfrdlova Z, Rektor I: Atypical hemispheric language dominance in left temporal lobe epilepsy as a result of the reorganization of language functions. **Epilepsy Behav** 4:414–419, 2003.
5. Chen HM, Varshney PK: Mutual information-based CT-MR brain image registration using generalized partial volume joint histogram estimation. **IEEE Trans Med Imaging** 22:1111–1119, 2003.

FIGURE 5. *A 40-year-old, left-handed woman with epilepsy. A, fMRI with the verb generation task showed activations predominantly in the right IFG and MFG. B, fMRI with the A/C categorization task demonstrated activations in the right MFG and the posterior STG. C, source localization of the late deflections on MEG showed predominant dipole clusters* (white squares) *in the right posterior temporal region. The left and right hemispheres showed 44 and 144 dipoles, respectively. D, three-dimensionally reconstructed MRI scans fused with activation of the verb generation-fMRI* (orange) *and dipoles of language-MEG* (blue). *After implantation of subdural electrodes* (gold), *cortical mapping was performed with 50Hz bipolar electrical stimulation. Stimulation with intensity of 7mA to the right IFG caused speech arrest* (white circles), *whereas stimulation to the posterior STG caused impairment of auditory comprehension and reading capability* (black circles).

6. FitzGerald DB, Cosgrove GR, Ronner S, Jiang H, Buchbinder BR, Belliveau JW, Rosen BR, Benson RR: Location of language in the cortex: A comparison between functional MR imaging and electrocortical stimulation. **AJNR Am J Neuroradiol** 18:1529–1539, 1997.
7. Holodny AI, Schulder M, Liu WC, Maldjian JA, Kalnin AJ: Decreased BOLD functional MR activation of the motor and sensory cortices adjacent to a glioblastoma multiforme: Implications for image-guided neurosurgery. **AJNR Am J Neuroradiol** 20:609–612, 1999.
8. Holodny AI, Schulder M, Ybasco A, Liu WC: Translocation of Broca's area to the contralateral hemisphere as the result of the growth of a left inferior frontal glioma. **J Comput Assist Tomogr** 26:941–943, 2002.
9. Janszky J, Ollech I, Jokeit H, Kontopoulou K, Mertens M, Pohlmann-Eden B, Ebner A, Woermann FG: Epileptic activity influences the lateralization of mesiotemporal fMRI activity. **Neurology** 63:1813–1817, 2004.
10. Kamada K, Houkin K, Iwasaki Y, Takeuchi F, Kuriki S, Mitsumori K, Sawamura Y: Rapid identification of the primary motor area by using magnetic resonance axonography. **J Neurosurg** 97:558–567, 2002.
11. Kamada K, Kober H, Saguer M, Moller M, Kaltenhauser M, Vieth J: Responses to silent Kanji reading of the native Japanese and German in task subtraction magnetoencephalography. **Brain Res Cogn Brain Res** 7:89–98, 1998.
12. Kamada K, Sawamura Y, Takeuchi F, Houkin K, Kawaguchi H, Iwasaki Y, Kuriki S: Gradual recovery from dyslexia and related serial magnetoencephalographic changes in the lexicosemantic centers after resection of a mesial temporal astrocytoma. Case report. **J Neurosurg** 100:1101–1106, 2004.
13. Kutas M, Hillyard SA: Reading senseless sentences: Brain potentials reflect semantic incongruity. **Science** 207:203–205, 1980.
14. Kutas M, Hillyard SA: Brain potentials during reading reflect word expectancy and semantic association. **Nature** 307:161–163, 1984.
15. Lehericy S, Biondi A, Sourour N, Vlaicu M, du Montcel ST, Cohen L, Vivas E, Capelle L, Faillot T, Casasco A, Le Bihan D, Marsault C: Arteriovenous brain malformations: Is functional MR imaging reliable for studying language reorganization in patients? Initial observations. **Radiology** 223:672–682, 2002.
16. Lehericy S, Cohen L, Bazin B, Samson S, Giacomini E, Rougetet R, Hertz-Pannier L, Le Bihan D, Marsault C, Baulac M: Functional MR evaluation of temporal and frontal language dominance compared with the Wada test. **Neurology** 54:1625–1633, 2000.
17. Nobre AC, Allison T, McCarthy G: Word recognition in the human inferior temporal lobe. **Nature** 372:260–263, 1994.
18. Oldfield RC: The assessment and analysis of handedness: The Edinburgh inventory. **Neuropsychologia** 9:97–113, 1971.
19. Papanicolaou AC, Simos PG, Breier JI, Zouridakis G, Willmore LJ, Wheless JW, Constantinou JE, Maggio WW, Gormley WB: Magnetoencephalographic mapping of the language-specific cortex. **J Neurosurg** 90:85–93, 1999.
20. Papanicolaou AC, Simos PG, Castillo EM, Breier JI, Sarkari S, Pataraia E, Billingsley RL, Buchanan S, Wheless J, Maggio V, Maggio WW: Magnetocephalography: A noninvasive alternative to the Wada procedure. **J Neurosurg** 100:867–876, 2004.
21. Petrovich NM, Holodny AI, Brennan CW, Gutin PH: Isolated translocation of Wernicke's area to the right hemisphere in a 62-year-man with a temporoparietal glioma. **AJNR Am J Neuroradiol** 25:130–133, 2004.
22. Pouratian N, Bookheimer SY, Rex DE, Martin NA, Toga AW: Utility of preoperative functional magnetic resonance imaging for identifying language cortices in patients with vascular malformations. **Neurosurg Focus** 13:E4, 2002.
23. Ries ML, Boop FA, Griebel ML, Zou P, Phillips NS, Johnson SC, Williams JP, Helton KJ, Ogg RJ: Functional MRI and Wada determination of language lateralization: A case of crossed dominance. **Epilepsia** 45:85–89, 2004.
24. Roux FE, Boulanouar K, Lotterie JA, Mejdoubi M, LeSage JP, Berry I: Language functional magnetic resonance imaging in preoperative assessment of language areas: Correlation with direct cortical stimulation. **Neurosurgery** 52:1335–1345, 2003.
25. Rutten GJ, Ramsey NF, van Rijen PC, Noordmans HJ, van Veelen CW: Development of a functional magnetic resonance imaging protocol for intraoperative localization of critical temporoparietal language areas. **Ann Neurol** 51:350–360, 2002.
26. Rutten GJ, Ramsey NF, van Rijen PC, van Veelen CW: Reproducibility of fMRI-determined language lateralization in individual subjects. **Brain Lang** 80:421–437, 2002.
27. Simos PG, Papanicolaou AC, Breier JI, Wheless JW, Constantinou JE, Gormley WB, Maggio WW: Localization of language-specific cortex by using magnetic source imaging and electrical stimulation mapping. **J Neurosurg** 91:787–796, 1999.
28. Woermann FG, Jokeit H, Luerding R, Freitag H, Schulz R, Guertler S, Okujava M, Wolf P, Tuxhorn I, Ebner A: Language lateralization by Wada test and fMRI in 100 patients with epilepsy. **Neurology** 61:699–701, 2003.
29. Yetkin FZ, Mueller WM, Morris GL, McAuliffe TL, Ulmer JL, Cox RW, Daniels DL, Haughton VM: Functional MR activation correlated with intraoperative cortical mapping. **AJNR Am J Neuroradiol** 18:1311–1315, 1997.

COMMENTS

This is an interesting article evaluating the complementary features of functional magnetic resonance imaging (fMRI) and magnetoencephalography (MEG) to assess language lateralization in 87 patients. Whereas any test of language lateralization is suspect if 100% correlation is found, the authors have carefully described their techniques and the analysis of results. It is quite apparent that fMRI with verb generation tasks is best at activating anterior language areas, whereas abstract versus concrete naming tasks can be less robust. This is a good article and a large experience worthy of publication.

G. Rees Cosgrove
Burlington, Massachusetts

The authors have applied fMRI and MEG techniques to localize speech function in a large number of patients with different brain lesions. They were able to supplement the two noninvasive tests with the Wada test in 80% of the patients. They were able to obtain useful data with the co-utilization of fMRI and MEG in 95.6% of the patients and found a somewhat surprisingly good match with the results of the Wada test in 100% of those. In the results section, the authors discuss a few differences to the localization of language areas by electrophysiological means. They point out the fact that atypical language dominance or bilateral language representation is more frequent in patients with chronic epilepsy than in those without epilepsy. This is an important fact not known to many neurosurgeons who are not ordinarily involved with epilepsy cases. The results of this study make it more likely that, in the future, the invasive Wada test procedure might be abolished in those institutions at which MEG is available. This constitutes a notable limitation of this noninvasive technique. If fMRI is used alone, the success rate for obtaining useful data is 84.6% for word generation tasks and only 67% for the abstract/concrete categorization task. This is quite an interesting study and the results are very promising; however, the limitations are not economical. A number of patients cannot complete all the tasks necessary for fMRI study, and MEG studies can be disturbed by eye movement artifacts. We look forward to other reports confirming these promising results.

Johannes Schramm
Bonn, Germany

The authors present some very interesting data in the realm of functional imaging to determine cerebral dominance for language. Currently, the standard modality for determining cerebral dominance is the venerable Wada test. In this study, the authors use both MEG and fMRI to determine language dominance based on activation in the inferior frontal gyrus and middle frontal gyrus using fMRI and dipole moments reflecting or indicating receptive language fields in the temporal lobe. As expected, they had some difficulty with the fMRI data owing to the underlying deficit in the patient, which suggests that fMRI is not always as good as one might expect in terms of determin-

ing cerebral dominance using a verb generation silent language task. We know that fMRI is not a good choice for defining receptive language fields that correspond to intraoperative stimulation mapping. However, when fMRI was used together with MEG, the authors were able to demonstrate 100% concordance with data from the Wada test. Thus, this is a very important study indicating that, in the near future, it may be possible to bypass the Wada test with these two powerful functional imaging modalities. That being said, not every institution is going to be able to obtain both of these functional tests. Therefore, it is unlikely that this strategy is going to replace Wada tests completely. Yet, this is a very important line of investigation and a novel observation that points out the frailties of functional imaging for cerebral dominance localization and the potential power when the different functional tests are combined.

Mitchel S. Berger
San Francisco, California

Portrait of James Figg (1695–1734), by William Hogarth, (1697–1764). Acknowledged in Britain as the "Father of Boxing," Figg popularized the sport with teaching and exhibitions and, following victories over all the other British contenders, declared himself "heavyweight champion of England" in 1719.

Int. J. Radiation Oncology Biol. Phys., Vol. 68, No. 5, pp. 1388–1395, 2007

0360-3016/07/$–see front matter

ELSEVIER

doi:10.1016/j.ijrobp.2007.03.048

CLINICAL INVESTIGATION **Brain**

NEUROCOGNITIVE FUNCTION OF PATIENTS WITH BRAIN METASTASIS WHO RECEIVED EITHER WHOLE BRAIN RADIOTHERAPY PLUS STEREOTACTIC RADIOSURGERY OR RADIOSURGERY ALONE

HIDEFUMI AOYAMA, M.D., PH.D.,[a] MASAO TAGO, M.D., PH.D.,[b] NORIO KATO, M.D.,[a] TATSUYA TOYODA, M.D., PH.D.,[c] MASAHIRO KENJYO, M.D., PH.D.,[d] SAEKO HIROTA, M.D., PH.D.,[e] HIROKI SHIOURA, M.D., PH.D.,[f] TAISUKE INOMATA, M.D., PH.D.,[g] ETSUO KUNIEDA, M.D., PH.D.,[h] KAZUSHIGE HAYAKAWA, M.D., PH.D.,[i] KEIICHI NAKAGAWA, M.D., PH.D.,[b] GEN KOBASHI, M.D., PH.D.,[j] AND HIROKI SHIRATO, M.D., PH.D.[a]

[a] Department of Radiology, Hokkaido University Graduate School of Medicine, Sapporo; [b] Department of Radiology, University of Tokyo Hospital, Tokyo; [c] Department of Radiology, Kanto Medical Center Nippon Telegraph and Telephone East Corporation, Tokyo; [d] Department of Radiology, Hiroshima University School of Medicine, Hiroshima; [e] Department of Radiology, Hyogo Medical Center for Adults, Akashi; [f] Department of Radiology, Izumisano General Hospital, Izumisano; [g] Department of Radiology, Osaka Medical College, Osaka; [h] Department of Radiology, Keio University School of Medicine, Tokyo; [i] Department of Radiology, Kitasato University School of Medicine, Sagamihara; and [j] Department of Global Health and Epidemiology, Division of Preventive Medicine, Hokkaido University Graduate School of Medicine, Sapporo, Japan

Purpose: To determine how the omission of whole brain radiotherapy (WBRT) affects the neurocognitive function of patients with one to four brain metastases who have been treated with stereotactic radiosurgery (SRS).
Methods and Materials: In a prospective randomized trial between WBRT+SRS and SRS alone for patients with one to four brain metastases, we assessed the neurocognitive function using the Mini-Mental State Examination (MMSE). Of the 132 enrolled patients, MMSE scores were available for 110.
Results: In the baseline MMSE analyses, statistically significant differences were observed for total tumor volume, extent of tumor edema, age, and Karnofsky performance status. Of the 92 patients who underwent the follow-up MMSE, 39 had a baseline MMSE score of ≤27 (17 in the WBRT+SRS group and 22 in the SRS-alone group). Improvements of ≥3 points in the MMSEs of 9 WBRT+SRS patients and 11 SRS-alone patients ($p = 0.85$) were observed. Of the 82 patients with a baseline MMSE score of ≥27 or whose baseline MMSE score was ≤26 but had improved to ≥27 after the initial brain treatment, the 12-, 24-, and 36-month actuarial free rate of the 3-point drop in the MMSE was 76.1%, 68.5%, and 14.7% in the WBRT+SRS group and 59.3%, 51.9%, and 51.9% in the SRS-alone group, respectively. The average duration until deterioration was 16.5 months in the WBRT+SRS group and 7.6 months in the SRS-alone group ($p = 0.05$).
Conclusion: The results of the present study have revealed that, for most brain metastatic patients, control of the brain tumor is the most important factor for stabilizing neurocognitive function. However, the long-term adverse effects of WBRT on neurocognitive function might not be negligible. © 2007 Elsevier Inc.

Brain metastasis, Radiosurgery, Whole brain radiotherapy, Neurocognitive function, Leukoencephalopathy.

INTRODUCTION

Whole brain radiotherapy (WBRT) has long been a mainstay of treatment of brain metastases. The role of WBRT is to control radiologically visualized tumors, as well as nonvisualized micrometastases. Stereotactic radiosurgery (SRS) is a method of delivering high doses of focal irradiation to a tumor while minimizing the irradiation to the adjacent normal tissue (1, 2). Beginning in the 1990s, it has become increasingly used worldwide for patients with no more than a few brain metastases. A recent prospective randomized trial from the Radiation Therapy Oncology Group (RTOG) showed a small, but significant, improvement in the survival of patients who had had up to three metastases with good prognostic factors when SRS was used in conjunction with WBRT (2).

Reprint requests to: Hidefumi Aoyama, M.D., Ph.D., Department of Radiology, Hokkaido University Graduate School of Medicine, North 15, West 7, Kita-ku, Sapporo 060-8638, Japan. Tel: (+81) 11-716-1161; Fax: (+81) 11-706-7876; E-mail: hao@radi.med.hokudai.ac.jp

Partly supported by a grant-in-aid for scientific research (Grant 18209039) from the Japanese Ministry of Education, Culture, Sports, Science, and Technology.

Conflict of interest: none.

Received Feb 19, 2007, and in revised form March 26, 2007. Accepted for publication March 27, 2007.

However, WBRT has several adverse effects. Acute adverse effects include nausea and headache, but they are generally limited in severity and duration. However, the late adverse effects are severe, progressive, and irreversible. They are caused by a syndrome called leukoencephalopathy, which is a structural alteration of cerebral white matter in which myelin suffers the most damage. Mild cases are typified by a chronic confusional state with inattention, memory loss, and emotional dysfunction. More severe cases produce major neurologic sequelae such as dementia, abulia, stupor, and coma. These symptoms usually develop 6–24 months after cranial RT. The degree of neurotoxicity resulting from WBRT correlates with the total dose received and with the time-dose-fractionation scheme (3). Because of the concern about leukoencephalopathy resulting from WBRT, treatment strategies relying on SRS alone have been increasingly used (4–7). However, the omission of WBRT from the initial brain management has resulted in a significant increase in brain tumor recurrence (6, 7). Regine *et al.* (8) reported that brain tumor recurrence could also be a cause of neurocognitive functional deterioration.

The present study from the Japanese Radiation Oncology Study Group Protocol 99-1 is the first prospective randomized trial comparing SRS alone and WBRT combined with SRS. The details of the results have been previously published (1). In brief, it was a multi-institutional prospective randomized trial comparing WBRT+SRS and SRS alone conducted in Japan between 1999 and 2003. The 132 patients were randomized to receive WBRT+SRS (n = 65) or SRS alone (n = 67) for brain metastases. The primary endpoint was survival. No significant difference between the groups was observed in survival or cause of death; however, patients in the SRS-alone group developed brain tumor recurrences significantly more frequently than did those in the WBRT+SRS group. No difference in the functional observation rate (Karnofsky performance status ≥70) was observed.

We also monitored neurocognitive function serially using the Mini-Mental State Examination (MMSE) (8–12). We present the results of our detailed analysis of neurocognitive function for this trial. This is the first report to compare the neurocognitive function of patients who underwent either SRS alone or WBRT+SRS.

METHODS AND MATERIALS

Randomization and treatment

Eligible patients had one to four brain metastases detected on enhanced magnetic resonance imaging, each <3 cm, and a good systemic performance status (Karnofsky performance status of ≥70). A total of 132 patients were randomized to receive WBRT+SRS (65 patients) or SRS alone (67 patients) for brain metastases. Each patient provided written informed consent before entry into the study. Randomization was performed at the Hokkaido University Hospital Data Center. A permuted-blocks randomization algorithm was used with a block size of four. A randomization sheet was created for each institution. Before randomization, the patients were stratified according to the following criteria: number of brain metastases (single vs. two to four), extent of extracranial disease (active vs. stable), and primary tumor site (lung vs. other). Extracranial disease was considered to be stable when the tumor had been clinically controlled for ≥6 months before the detection of brain metastases. The WBRT schedule was 30 Gy in 10 fractions within 2–2.5 weeks. WBRT proceeded to SRS in patients assigned to the WBRT+SRS group. The SRS dose was prescribed to the tumor margin. Metastases with a maximal diameter of ≤2 cm were treated with 22–25 Gy, and those >2 cm were treated with 18–20 Gy. The dose was reduced by 30% when the treatment was combined with WBRT (1).

Assessment of neurocognitive function

Neurocognitive function was assessed using the MMSE (8–12). The MMSE is a short, standardized tool to grade cognitive function. The examination begins with an assessment of orientation to place and time. A maximum of 10 points can be obtained in this section. The memory test has the subject immediately repeat the name of three objects presented orally. The subject then subtracts 7s serially from 100 and is subsequently asked to recall the three items previously repeated. The final section evaluates aphasia and apraxia by testing naming, repetition, compliance with a three-step command, comprehension of written words, writing, and copying a drawing, for a total of 9 points in this section. The maximal score that can be obtained for the entire MMSE is 30 points (10–12). Physicians administered the MMSE before or during the brain treatment, again at 1 and 3 months after treatment and, if possible, every 3 months thereafter. The factors included in the analyses were the number of brain metastases on contrast-enhanced magnetic resonance imaging (MRI), the total volume of brain metastases, and the degree of brain edema on T_2-weighted MRI. Brain edema was scored from Grade 0 to 2. Patients with Grade 0 had no edema; those with Grade 1 had edema limited to less than one-half of one hemisphere, and those with Grade 2 had edema exceeding one-half of one hemisphere.

For the analysis of the post-treatment changes in the MMSE, patients for whom no follow-up MMSEs were available were excluded. A statistically meaningful change was defined as a three-point change in the MMSE score (8, 12). Although this criterion was thought to be potentially less conservative, owing to the possibility of missing a "meaningful" change in the MMSE score (13), it might be a more reliable change index (8, 12). In addition, a score of ≤26 was defined as abnormal (8). MRI findings regarding leukoencephalopathy were also assessed according to the criterion in the National Cancer Institute Common Toxicity Criteria, version 2.0, and correlated with the change in MMSE score (14). Tumor progression was scored when the tumor size had increased by at least 25% using the measurement of the perpendicular diameters (1).

Statistical analysis

The MMSE score was summarized as an average. Because of a ceiling effect and the clustering of values at 30, the data were not normally distributed. The Wilcoxon rank sum test was used to compare the mean values. The chi-square test was used to determine the relationship between two categorical variables, and Fisher's exact test was used when small cell sizes were encountered in 2 × 2 contingency tables. Univariate analyses were performed using the Kaplan-Meier method, and we used the log–rank test to compare differences between the groups. A two-sided p value of ≤0.05 was considered to reflect statistical significance. All statistical analyses were initially performed by a physician (H.A.) using a commercial statistical software package (StatView, version 5.0J, SAS Institute, Cary, NC), and all results were verified by a statistician

(G.K.) using a different software package (Statistical Analysis Systems, version 9.1, SAS Institute Japan, Tokyo, Japan).

RESULTS

Baseline MMSE

The pretreatment MMSE was available for 99 patients. MMSE data during the treatment were obtained for 11 additional patients. Those data, from 110 (83%) of the 132 patients enrolled in the study, constituted the "baseline" MMSE data and were used for the analysis (Fig. 1). The characteristics of those 110 patients are listed in Table 1 by treatment group. No statistically significant differences were found between the two groups. A comparison of the MMSE scores according to the patient characteristics is summarized in Table 2. The average baseline MMSE did not differ significantly between treatment groups ($p = 0.47$). Statistically significant differences were observed in the total tumor volume of brain metastases (<3 vs. ≥3 cm^3), extent of tumor edema (Grade 0-1 vs. Grade 2), age (<65 vs. ≥65 years), and Karnofsky performance status (70–80 vs. 90–100). The number of brain metastases was not a significant factor.

Post-treatment change in MMSE

Post-treatment improvement in MMSE. Follow-up MMSEs were given to 92 patients a median of 2.5 times (range, 1–17). The median follow-up period was 5.3 months (average, 11.0; range, 0.7–58.7). Of those 92 patients, 39 (17 in the WBRT+SRS group and 22 in the SRS-alone group) had a baseline MMSE score of ≤27. The 53 patients who had a baseline MMSE score of 28–30 were excluded from this analysis because an improvement of ≥3 points could not be expected (ceiling effect). The mean ± standard deviation MMSE value was 24.9 ± 3.3 in the WBRT+SRS group and 25.3 ± 2.1 in the SRS-alone group ($p = 0.65$). An improvement in MMSE of ≥3 points was observed in 20 (51%) of the 39 patients after the initial brain treatment. No statistically significant difference was found between the two treatment groups: 9 of 17 in the WBRT+SRS group and 11 of 22 in the SRS-alone group (chi-square = 0.03, $p = 0.85$). The improvement was observed at the mean of 6.0 ± 5.9 months in the WBRT+SRS group and 3.6 ± 2.8 months in the SRS-alone group ($p = 0.24$). Three patients experienced a worsening of MMSE (deterioration by ≥3 points) without improvement. The remaining 16 patients did not show a change of ≥3 points in their MMSE scores.

Post-treatment deterioration of MMSE. Included in this analysis were patients who had a baseline MMSE score of ≥27 ($n = 65$) and those whose baseline MMSE score was ≤26 but improved to ≥27 ($n = 17$) after the initial brain treatment. Because we found that some patients experience improvement in the MMSE after the initial brain treatment, we used the best MMSE score minus the deteriorated MMSE score for the change in MMSE for this analysis. The Kaplan-Meier curves of the patients who did not have a 3-point deterioration in the MMSE score in each treatment group are shown in Fig. 2a. No statistically significant difference was found by log–rank test ($p = 0.73$). Deterioration of the MMSE score occurred in 14 of 36 patients in the WBRT+SRS group and 12 of 46 in the SRS-alone group (chi-square =1.52, $p = 0.21$). However, the time until the deterioration was marginally different between the two groups. Deterioration was observed at an average of 13.6 months (median, 12.0; range, 1.8–31.1) in the WBRT+SRS group and 6.8 months (median, 6.6; range, 1.6–12.9) in the SRS-alone group ($p = 0.05$). The deterioration was presumably attributed to brain tumor recurrence in 3 and 11 patients in the WBRT+SRS and SRS-alone groups, respectively ($p < 0.0001$). The deterioration was either clinically or radiologically attributed to a toxic radiation event in 5 and 0 patients in the WBRT+SRS and SRS-alone groups, respectively. The cause was unclear in the remaining 7 patients. An additional follow-up MMSE after the 3-point decrease was available for 10 of 26 patients. Of those 10, an improvement of ≥3 points was observed in 7 (5 in the WBRT+SRS group and 2 in the SRS-alone group). Of the 7 patient, 2 underwent salvage brain treatment (1 with SRS and 1 with surgery). The other 5 patients received only close observation or best supportive care, including steroid administration. Figure 2b shows the

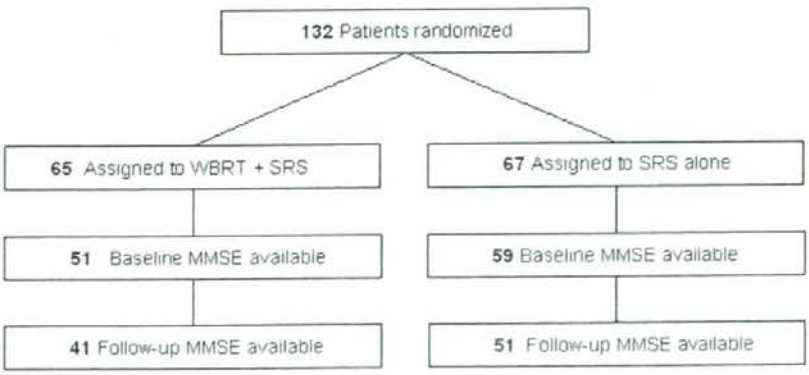

Fig. 1. Flow chart of study participants. WBRT = whole brain radiotherapy; SRS = stereotactic radiosurgery; MMSE = Mini-Mental State Examination.

Table 1. Baseline patient characteristics

Characteristic	WBRT+SRS (n = 51)	SRS (n = 59)	p
Age at diagnosis (y)			0.71
Median	65	64	
Range	36–78	33–81	
<65 y	25 (49)	31 (52)	
≥65 y	26 (51)	28 (48)	
Gender			0.37
Men	36 (71)	46 (78)	
Women	15 (29)	13 (22)	
Karnofsky performance status			0.22
70–80	24 (47)	21 (36)	
90–100	27 (53)	38 (64)	
No. of brain metastases			0.82
1	27 (53)	30 (51)	
2–4	24 (47)	29 (49)	
Brain edema			0.63
Grade 0	13 (25)	14 (24)	
Grade 1	29 (57)	38 (64)	
Grade 2	9 (18)	7 (12)	
Total volume of brain metastases (cm^3)			0.67
<3	23 (45)	29 (49)	
≥3	28 (55)	30 (51)	
Primary tumor site			0.71
Lung	32 (63)	39 (66)	
Other	19 (37)	20 (34)	
Primary tumor status			0.54
Stable	23 (45)	30 (51)	
Active	28 (55)	29 (49)	
Extracranial metastases			0.40
Stable	35 (69)	36 (61)	
Active	16 (31)	23 (39)	

Abbreviations: WBRT = whole brain radiotherapy; SRS = stereotactic radiosurgery.

Data presented as number of patients, with percentages in parentheses, unless otherwise noted.

Table 2. Analysis of baseline MMSE score and associated factors

Variable	n	Average (SD)	p (Mann-Whitney U test)
Treatment group			0.86
WBRT+SRS	51	26.7 (3.3)	
SRS alone	59	27.1 (2.9)	
Age at diagnosis (y)			0.001
<65	56	27.9 (2.0)	
≥65	54	25.9 (3.7)	
Gender			0.33
Men	82	26.7 (3.3)	
Women	28	27.6 (2.1)	
Karnofsky performance status			0.0002
70–80	45	25.5 (3.8)	
90–100	65	27.9 (1.9)	
No. of brain metastases			0.29
1	57	27.4 (2.3)	
2–4	53	26.4 (3.7)	
Brain edema			
Grade 0-1	94	27.2 (2.8)	
Grade 2	16	25.0 (4.2)	
Total volume of brain metastases (cm^3)			0.01
<3	52	27.8 (1.9)	
≥3	58	26.1 (3.7)	
Primary tumor site			0.86
Lung	71	26.9 (3.2)	
Other	39	27.0 (2.9)	
Extracranial disease			0.96
Stable	23	27.6 (2.2)	
Active	87	27.2 (2.2)	

Abbreviations: MMSE = Mini-Mental State Examination; SD = standard deviation; other abbreviations as in Table 1.

Kaplan-Meier curves of patients free of MMSE deterioration when the first event in a decrease was not counted if the MMSE showed significant recovery with additional follow-up. The 12-, 24-, and 36-month actuarial free rate of a second event in the 3-point decrease in the MMSE score was 76.1% (95% confidence interval [CI], 58.7–93.5), 68.5% (95% CI, 47.3–89.7), and 14.7% (95% CI, 0–39.0) in the WBRT+SRS group and 59.3% (95% CI, 37.5–81.1), 51.9% (95% CI, 28.6–75.2), and 51.9% (95% CI, 28.6–75.2) in the SRS-alone group, respectively. Although the difference was not significant by the log–rank test ($p = 0.79$), the separation of the two curves at between 12 and 24 months became wider than that in Fig. 2a. The average duration until deterioration was 16.5 months (median, 15.8; range, 1.8–34.5) in the WBRT+SRS group and 7.6 months (median, 7.4; range, 1.6–12.9) in the SRS-alone group ($p = 0.05$).

Figure 2c shows the actuarial rate of subjects free from a decrease in the MMSE score to ≤26. An event of a decrease to ≤26 was counted as an event unless the MMSE score recovered to ≥27 with additional follow-up. The 12-, 24-, and 36-month actuarial MMSE preservation rate (≥27) was 78.8% (95% CI, 61.6–96.0), 78.8% (95% CI, 61.6–96.0), and 22.5% (95% CI, 0–49.4) in the WBRT+SRS group and 53.3% (95% CI, 32.9–73.7), 42.6% (95% CI, 17.9–67.3), and 42.6% (95% CI, 17.9–67.3) in the SRS-alone group, respectively ($p = 0.46$). The separation of the two curves at between 12 and 24 months after treatment became more prominent than that in Fig. 2b. This fact might indicate that WBRT was effective at preventing the deterioration of neurocognitive function resulting from brain tumor recurrence in an early phase after treatment. However, WBRT could be a cause of continuous deterioration of neurocognitive function in long-term survivors.

The relationship between the MRI findings of leukoencephalopathy using the National Cancer Institute Common Toxicity Criteria, version 2, and clinical manifestations was also evaluated. Abnormal MRI-determined leukoencephalopathy was seen in 7 patients (Grade 1 in 2 patients, Grade 2 in 4, and Grade 3 in 1). All 7 patients were in the WBRT+SRS group. Four of them (Grade 1 in 1 patient, Grade 2 in 2, and Grade 3 in 1) experienced a clinically significant decrease in the MMSE score (≥3 points). The other 3 patients (Grade 1 in 1 and Grade 2 in 2) did not experience a significant decrease in the MMSE score. Fig. 3 shows illustrative MRI scans of 2 patients with different clinical courses.

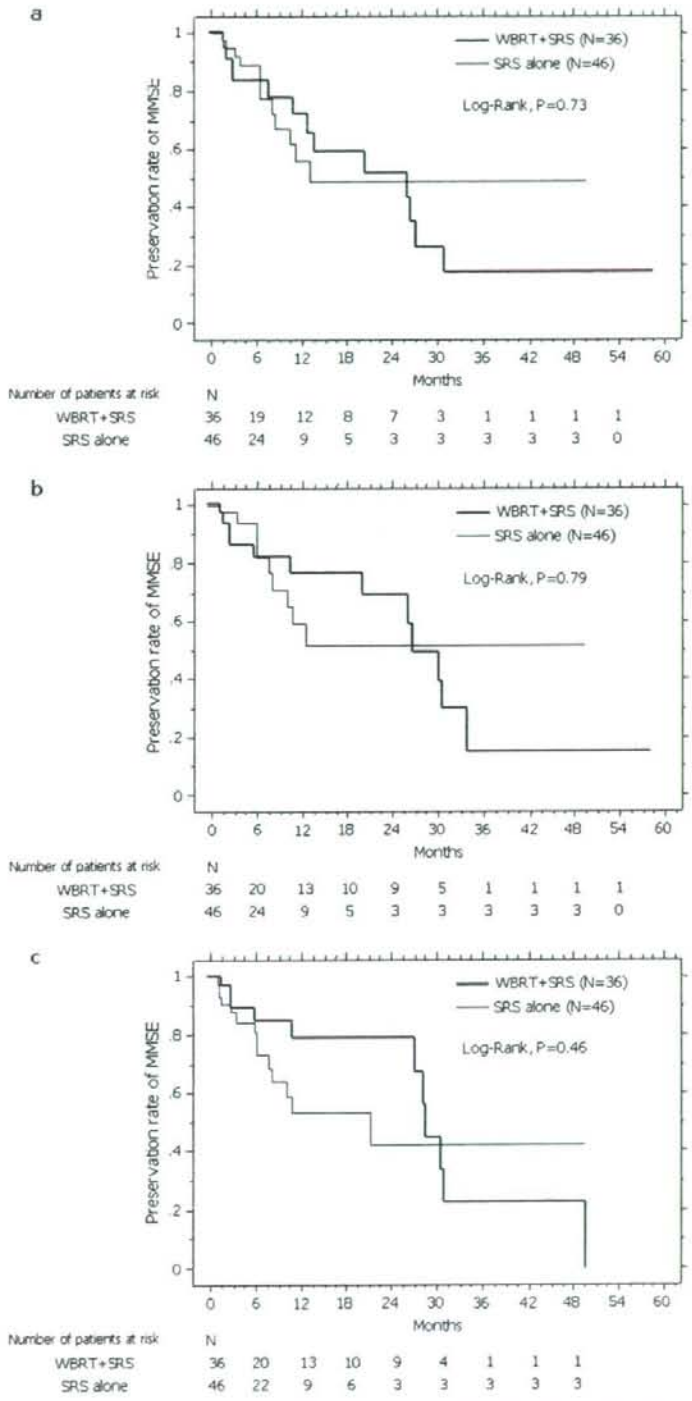

Fig. 2. (a) Actuarial curves of subjects free from 3-point decrease in Mini-Mental State Examination (MMSE). (b) Actuarial curves of subjects free from second 3-point decrease in MMSE. (c) Actuarial rate of subjects free from decrease of MMSE to ≤26. WBRT = whole brain radiotherapy; SRS = stereotactic radiosurgery.

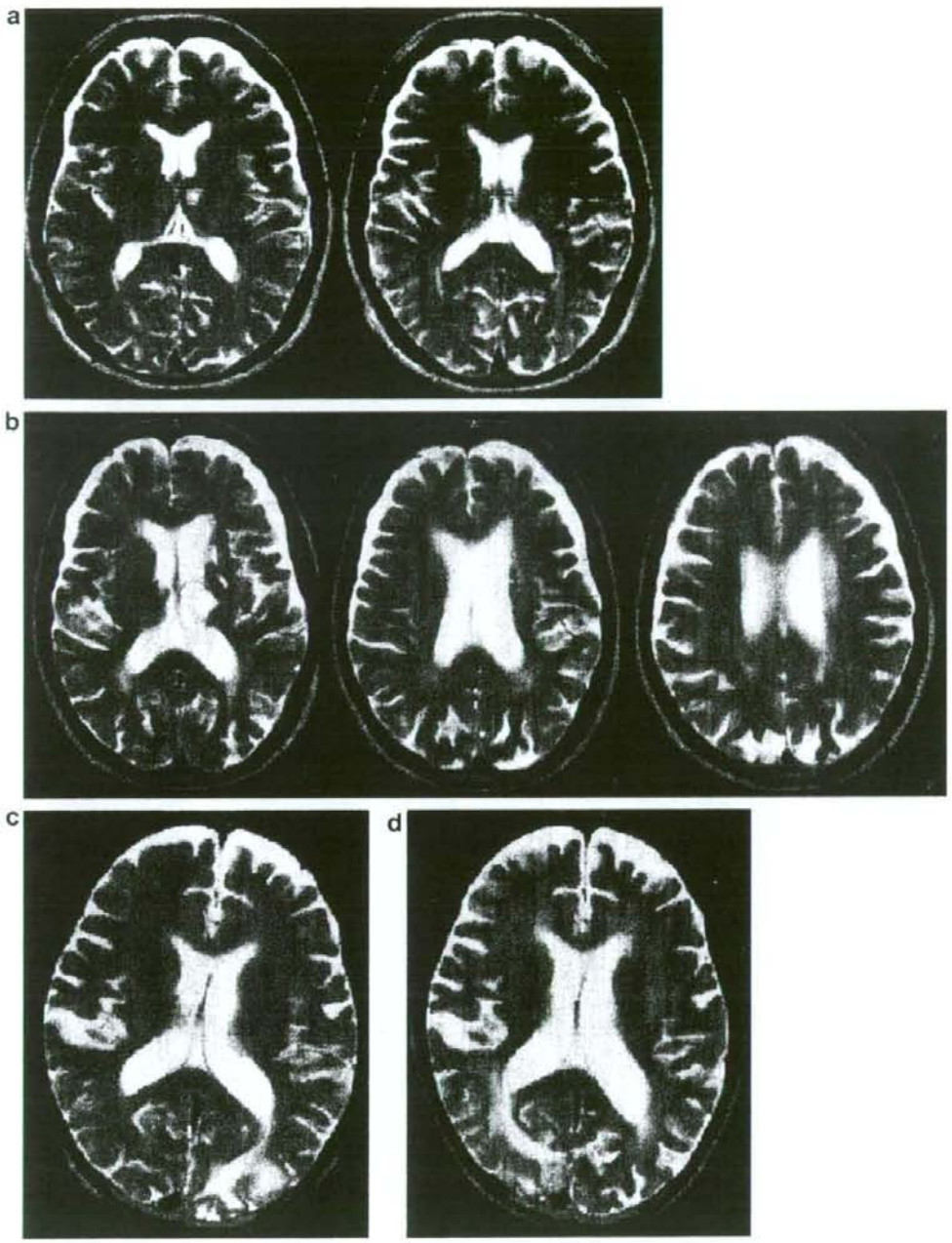

Fig. 3. (a) Pretreatment T_2-weighted magnetic resonance imaging (MRI) study of Patient 1, who then underwent whole brain radiotherapy (WBRT) plus stereotactic radiosurgery (SRS). (b) T_2-weighted MRI scan of Patient 1 at 46.6 months after initial brain treatment. (c) Pretreatment T_2-weighted MRI study of Patient 2, who then underwent WBRT plus SRS. (d) T_2-weighted MRI scan of Patient 2 at 15 months after initial brain treatment.

Patient 1 experienced Grade 3 radiologic leukoencephalopathy without tumor recurrence at 47 months after WBRT+SRS (Fig. 3a, b). This patient had a baseline MMSE score of 29 and a best score of 30 at 7 months after RT. She experienced a continuous decrease in the MMSE score after a transient recovery, and her last MMSE score, at 47 months, was 21. Patient 2 experienced Grade 2 radiologic leukoencephalopathy at 15 months after WBRT+SRS. His baseline MMSE score was 29 and his final score, at 15 months, was 29 (Fig. 3c, d).

DISCUSSION

The MMSE is the most frequently used and established tool for assessing the neurocognitive function of patients with brain tumors (7–13). The importance of MMSE in the treatment of patients with brain metastases, as well as in those with low-grade glioma, has been reported by Murray *et al.* (9) and Brown *et al.* (10). Murray *et al.* (9) assessed the MMSE scores of 182 patients with brain metastases who were treated with WBRT to 30 Gy in 10 fractions among 445 patients enrolled in a RTOG study (RTOG 91-04), in which 30 Gy in 10 fractions was compared with accelerated hyperfractionation of 54.4 Gy (1.6 Gy twice daily). They reported that patients who had low MMSE score (≤23) had a worse prognosis than those with greater MMSE scores. In 88 patients who had a baseline MMSE score of ≤29, 48 (54.5%) demonstrated an improvement in the MMSE score at a follow-up visit. Regine *et al.* (8) evaluated 309 patients whose MMSE scores were available among 445 patients who were enrolled in RTOG 91-04. They found that control of the brain tumor had a significant impact on the maintenance of the MMSE scores. At 3 months, the average change in MMSE score was a decline of 0.5 for those whose brain metastases were radiologically controlled compared with a decline of 6.3 for those with uncontrolled brain metastases ($p = 0.02$). One of the shortcomings of their report was that they evaluated the change in MMSE only at 3 months after brain treatment; therefore, the long-term effect of WBRT was not fully investigated. In the present study, we found some important factors that might affect a patient's baseline MMSE score. The number of brain metastases was not a significant factor affecting the baseline MMSE score, but tumor volume (≥3 cm^3) and degree of edema (one-half of one hemisphere or more) were significant factors. More importantly, 51% of patients who had an MMSE score of ≤27 experienced significant improvement in the MMSE score at a median of 2.7 months after treatment, regardless of which treatment they had initially received. This finding supports the findings reported by Murray *et al.* (9).

Another important finding of the present study was the continuous decrease in MMSE score in patients who underwent WBRT initially, although WBRT was not a cause of neurocognitive deterioration for most brain metastatic patients. Patients who received WBRT combined with SRS experienced a stable MMSE score for approximately 2 years after treatment, perhaps because of the preventative effect on brain tumor recurrence compared with SRS alone. Considering that the median survival of patients with brain metastases is about 7 months, this prevention effect when WBRT is included in the initial management is beneficial for most brain metastatic patients. Nevertheless, the continuous deterioration of neurocognitive function for long-term survivors who underwent WBRT should not be neglected.

In addition, the MRI findings suggestive of leukoencephalopathy were useful only for patients who experienced severe neurocognitive dysfunction. Most patients who had Grade 1-2 radiologic leukoencephalopathy did not show clinically meaningful signs of neurocognitive dysfunction as assessed by the MMSE. This is consistent with the findings of Fujii *et al.* (15). They evaluated the white matter changes on MRI after WBRT in 24 patients. Although 12 patients (50%) developed radiologic Grade 3 (large confluent areas) or worse leukoencephalopathy, only 6 of these 12 patients had clinical abnormalities such as dementia, depression, and speech impairment. However, the true incidence of neurocognitive deterioration is not well understood. In patients with small cell carcinoma of the lung whose primary tumor is in complete remission, prophylactic cranial irradiation (PCI) using WBRT is becoming a standard treatment (16). van de Pol *et al.* (17) assessed late neurologic toxicity in 7 patients who received PCI and survived ≥2 years. The memory decline was insidious and started within 6 months after the termination of therapy in 4 patients and after 2 years in 2 patients (17). Stuschke *et al.* (18) reported that patients treated with PCI had higher grade white matter abnormalities than patients who were not treated with PCI, as detected by T_2-weighted MRI ($p = 0.04$). Grade 4 white matter abnormalities were detected in 2 of 9 patients treated with PCI and in 0 of 4 patients not treated with PCI (18). Cull *et al.* (19) reported the frequency of neurocognitive impairment in 52 patients who received PCI and survived >2 years. They evaluated neurocognitive function using four different methods: the Williams delayed recall test, the Digit symbol, the Complex figure test, and Trials A and B. No impairment in any of these tests was observed in 19% of patients. Impairment was observed with one test in 27%, two tests in 22%, three tests in 25%, and all four tests in 7% (19). These findings indicate that WBRT frequently accompanies neurocognitive impairment in long-term survivors.

Although our findings are of interest, our report was not without limitations. First, we did not monitor the use of corticosteroids, which could potentially influence neurocognitive function. Second, we used MMSE as the sole measurement of neurocognitive function; however, the MMSE has been criticized for having low specificity and sensitivity (20). Recently, the RTOG began using a "neurocognitive battery" of several assessment tools (21–24). Mehta *et al.* (21, 22) suggested that this battery is feasible for use in clinical trials and could detect small changes in neurocognitive function that the MMSE alone could not detect. Nevertheless, we believe the present findings are valuable and that the MMSE is still a useful tool to examine neurocognitive function in trials in which neurocognitive function is not the primary endpoint. No established effective treatment is available for neurocognitive deterioration after WBRT. Recently, Shaw *et al.* (25) reported that donepezil, a drug developed for Alzheimer's disease, has a positive effect on cognitive function; however, additional investigation is necessary to establish this drug's potential role in relation to WBRT.

CONCLUSION

The results of the present study have revealed that the control of brain tumors is the most important factor in stabilizing

neurocognitive function for most brain metastatic patients. However, the long-term adverse effect on neurocognitive function might not be negligible. Therefore, the development of a method to identify those patients who are less likely to experience brain tumor recurrence, as well as additional investigation to establish an optimal schedule of WBRT when combined with SRS, are important steps toward the refinement of the treatment of brain metastases.

REFERENCES

1. Aoyama H, Shirato H, Tago M, *et al.* Stereotactic radiosurgery plus whole-brain radiation therapy vs. stereotactic radiosurgery alone for treatment of brain metastases: A randomized controlled trial. *JAMA* 2006;295:2483–2491.
2. Andrews DW, Scott CB, Sperduto PW, *et al.* Whole brain radiation therapy with or without stereotactic radiosurgery boost for patients with one to three brain metastases: Phase III results of the RTOG 9508 randomised trial. *Lancet* 2004;363:1665–1672.
3. Filley CM, Kleinschmidt-DeMasters BK. Toxic leukoencephalopathy. *N Engl J Med* 2001;345:425–432.
4. Hasegawa T, Kondziolka D, Flickinger JC, *et al.* Brain metastases treated with radiosurgery alone: An alternative to whole brain radiotherapy? *Neurosurgery* 2003;52:1318–1326.
5. Yamamoto M, Ide M, Nishio S, *et al.* Gamma knife radiosurgery for numerous brain metastases: Is this a safe treatment? *Int J Radiat Oncol Biol Phys* 2002;53:1279–1283.
6. Sneed PK, Suh JH, Goetsch SJ, *et al.* A multi-institutional review of radiosurgery alone vs. radiosurgery with whole brain radiotherapy as the initial management of brain metastases. *Int J Radiat Oncol Biol Phys* 2002;53:519–526.
7. Aoyama H, Shirato H, Onimaru R, *et al.* Hypofractionated stereotactic radiotherapy alone without whole brain irradiation for patients with solitary and oligo brain metastasis using noninvasive fixation of the skull. *Int J Radiat Oncol Biol Phys* 2003;56:793–800.
8. Regine WF, Scott C, Murray K, *et al.* Neurocognitive outcome in brain metastases patients treated with accelerated-fractionation vs. accelerated-hyperfractionated radiotherapy: An analysis from Radiation Therapy Oncology Group Study 91-04. *Int J Radiat Oncol Biol Phys* 2001;51:711–717.
9. Murray KJ, Scott C, Zachariah B, *et al.* Importance of the mini-mental status examination in the treatment of patients with brain metastases: A report from the Radiation Therapy Oncology Group protocol 91-04. *Int J Radiat Oncol Biol Phys* 2000;48: 59–64.
10. Brown PD, Buckner JC, O'Fallon JR, *et al.* Effects of radiotherapy on cognitive function in patients with low-grade glioma measured by the Folstein Mini-Mental State Examination. *J Clin Oncol* 2003;21:2519–2524.
11. Folstein MF, Folstein SE, McHugh PR. "Mini-mental state": A practical method for grading the cognitive state of patients for the clinician. *J Psychiatr Res* 1975;12:189–198.
12. Crum RM, Anthony JC, Bassett SS, *et al.* Population-based norms for the Mini-Mental State Examination by age and educational level. *JAMA* 1993;269:2386–2391.
13. Temkin NR, Heaton RK, Grant I, *et al.* Detecting significant change in neuropsychological test performance: A comparison of four models. *J Int Neuropsychol Soc* 1999;5:357–369.
14. RTOG/EORTC late radiation morbidity scoring schema. Available at: http://www.rtog.org/members/toxicity/late.html. Accessed June 15, 1999.
15. Fujii O, Tsujino K, Soejima T, *et al.* White matter changes on magnetic resonance imaging following whole-brain radiotherapy for brain metastases. *Radiat Med* 2006;24:345–350.
16. Auperin A, Arriagada R, Pignon JP, *et al.*, for the Prophylactic Cranial Irradiation Overview Collaborative Group. Prophylactic cranial irradiation for patients with small-cell lung cancer in complete remission. *N Engl J Med* 1999;341:476–484.
17. van de Pol M, ten Velde GP, Wilmink JT, *et al.* Efficacy and safety of prophylactic cranial irradiation in patients with small cell lung cancer. *J Neurooncol* 1997;35:153–160.
18. Stuschke M, Eberhardt W, Pottgen C, *et al.* Prophylactic cranial irradiation in locally advanced non-small-cell lung cancer after multimodality treatment: Long-term follow-up and investigations of late neuropsychologic effects. *J Clin Oncol* 1999;17: 2700–2709.
19. Cull A, Gregor A, Hopwood P, *et al.* Neurological and cognitive impairment in long-term survivors of small cell lung cancer. *Eur J Cancer* 1994;30:1067–1074.
20. Meyers CA, Wefel JS. The use of the Mini-Mental State Examination to assess cognitive functioning in cancer trials: No ifs, ands, or buts, or sensitivity. *J Clin Oncol* 2003;21:3557–3558.
21. Mehta MP, Shapiro WR, Glantz MJ, *et al.* Lead-in phase to randomized trial of motexafin gadolinium and whole brain radiation for patients with brain metastases: Centralized assessment of magnetic resonance imaging, neurocognitive, and neurologic end points. *J Clin Oncol* 2002;20:3445–3453.
22. Mehta MP, Rodrigus P, Terhaard CH, *et al.* Survival and neurologic outcomes in a randomized trial of motexafin gadolinium and whole-brain radiation therapy in brain metastases. *J Clin Oncol* 2003;21:2529–2536.
23. Meyers CA, Smith JA, Bezjak A, *et al.* Neurocognitive function and progression in patients with brain metastases treated with whole brain radiation and motexafin gadolinium: Results of a randomized phase III trial. *J Clin Oncol* 2004;22:157–165.
24. Regine WF, Schmitt FA, Scott CB, *et al.* Feasibility of neurocognitive outcome evaluations in patients with brain metastases in a multi-institutional cooperative group setting: Results of Radiation Therapy Oncology Group trial BR-0018. *Int J Radiat Oncol Biol Phys* 2004;58:1346–1352.
25. Shaw EG, Rosdhal R, D'Agostino RB Jr., *et al.* Phase II study of donepezil in irradiated brain tumor patients: Effect on cognitive function, mood, and quality of life. *J Clin Oncol* 2006;24: 1415–1420.

Radiat Med (2007) 25:430–431
DOI 10.1007/s11604-007-0168-9

LETTER TO THE EDITOR

Matrixmetalloproteinases: up-regulated in subclones that survived 10-Gy irradiation

Takeshi Nishioka · Motoaki Yasuda · Kaori Tsutsumi
Hisashi Haga · Hiroki Shirato

Received: May 14, 2007 / Accepted: June 29, 2007

We report an interesting finding regarding the mRNA expression pattern of cell lines that survived 10-Gy irradiation. According to the linear quadratic model in a textbook, the survival curve shows a straight line at high-dose areas, meaning that cells are killed at a constant rate. The model explains that there are two types of killing: α-killing, which is a function of dose D, and β-killing, which is a function of D^2. This is a kind of modified version of a hit model wherein some percentage of cells remain intact after irradiation.

We used mouse fibrosarcoma cells (QRsP, p53 wild type); 1×10^4 cells were exposed to 10 Gy. At day 12, we harvested 6 of about 30 colonies and established them as QRsPIR-1 to QUsPIR-6. cDNA microarray analysis was performed for the parental QRsP and QRsPIR-1. The pattern was significantly different between the two, suggesting that the cells that survived were not intact. Rather, they had a more aggressive nature than the parental QRsP: matrix metalloproteinase (MMP)13 (collagenase) and MMP3 were significantly up-regulated (26-fold and 23-fold, respectively). These results encouraged us to perform an in vivo study in which 2×10^4 cells were injected subcutaneously into the flanks of C57BL/6 mice (five animals each). At day 28, a large tumor mass was palpated in each of the five mice for QRSPIR-1. In contrast, only two mice developed a tumor mass of the parental QRsP. To form a tumor mass, degradation of surrounding tissue (mainly collagen) must be done. Our findings are quite revealing in this regard.

To see whether up-regulation of MMP is a rare event, we performed cDNA analysis for QRsPIR-5 and an in vitro 10-Gy irradiation experiment for human lung adenocarcinoma H1299 (p53 mutant) and human lung carcinoma A549 (p53 wild type) in a similar manner. Interestingly, MMP13 and MMP3 were up-regulated 4.0- and 6.4-fold, respectively, for QRsPIR-5. Although the changes were not as significant as for QRsPIR-1, the values were still large compared to other published DNA array data. We randomly selected IR-1 and IR-5 for array analysis. (other IR clones were left untouched because of the high cost of each array analysis, and it is possible that these other IR clones would have a similar pattern if we had performed the analysis on them.) MMP1 (collagenase) was up-regulated 4.4-fold and 2.0-fold for H1299-IR and A549-IR, respectively. In A549-IR, MMP7 (matrilysin) was also up-regulated 2.8-fold.

It should be emphasized that none of the MMP family was included in the down-regulated gene lists of our four array analyses. Recently, it has been reported that MMPs not only play an important role in tumor invasion but also enhance cell motility,[1–3] both of which are important characteristics of malignant tumor cells. In fact, a cell

T. Nishioka (✉) · K. Tsutsumi
Laboratory of Radiation Therapy, School of Medicine, Hokkaido University, N12W5, Kita-ku, Sapporo 060-0812, Japan
Tel./Fax +81-11-706-3411
e-mail: trout@radi.med.hokudai.ac.jp

M. Yasuda
Department of Oral Pathobiological Science, Graduate School of Dental Medicine, Hokkaido University, Sapporo, Japan

H. Haga
Division of Biological Sciences, Graduate School of Science, Hokkaido University, Sapporo, Japan

H. Shirato
Department of Radiology, Graduate School of Medicine, Hokkaido University, Sapporo, Japan

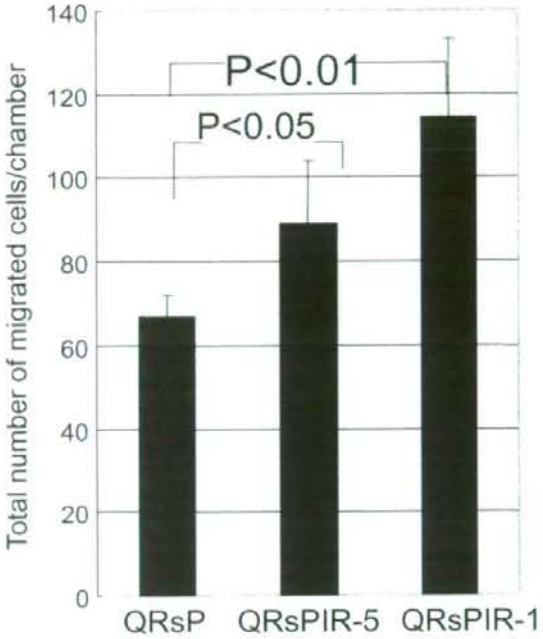

Fig. 1. Boyden chamber cell motility assay

motility assay using the Boyden chamber demonstrated increased cell motility for IR clones (Fig. 1). Cell motility was higher for QRsPIR-1 than for QRsPIR-5, which implies that MMPs are associated with cell movement.

In conclusion, all of our four cDNA array analyses showed up-regulation of MMPs. Irradiation is an effective means of cancer therapy, but it should be taken into consideration that surviving cells acquire a more aggressive nature.

References

1. López-Rivera E, Lizarbe TR, Martinez-Moreno M, López-Novoa JM, Rodriguez-Barbero A, et al. Matrix metalloproteinase 13 mediates nitric oxide activation of endothelial cell migration. Proc Natl Acad Sci U S A 2005;102:3685–90.
2. Sossey-Alaoui K, Ranalli TA, Li X, Bakin AV, Cowell JK. WAVE3 promotes cell motility and invasion through the regulation of MMP-1, MMP-3, and MMP-9 expression. Exp Cell Res 2005;308:135–45.
3. Remy L, Trespeuch C, Bachy S, Scoazec JY, Rousselle P. Matrilysin 1 influences colon carcinoma cell migration by cleavage of the laminin-5 beta3 chain. Cancer Res 2006;66:11228–37.

Int. J. Radiation Oncology Biol. Phys., Vol. 69, No. 2, pp. 376–380, 2007

0360-3016/07/$–see front matter

ELSEVIER

doi:10.1016/j.ijrobp.2007.03.042

CLINICAL INVESTIGATION **Liver**

INTERCEPTING RADIOTHERAPY USING A REAL-TIME TUMOR-TRACKING RADIOTHERAPY SYSTEM FOR HIGHLY SELECTED PATIENTS WITH HEPATOCELLULAR CARCINOMA UNRESECTABLE WITH OTHER MODALITIES

Hiroshi Taguchi, M.D.,* Yusuke Sakuhara, M.D.,* Shuhei Hige, M.D.,† Kei Kitamura, M.D.,* Yasuhiro Osaka, M.D.,* Daisuke Abo, M.D.,* Daichi Uchida, M.D.,* Akihiro Sawada, M.D.,* Toshiya Kamiyama, M.D.,‡ Tadashi Shimizu, M.D.,* Hiroki Shirato, M.D.,* and Kazuo Miyasaka, M.D.*

Departments of *Radiology, †Gastroenterology, and ‡General Surgery, Hokkaido University School of Medicine, Sapporo, Japan

Purpose: To assess the clinical outcome of intercepting radiotherapy, in which radiotherapy is delivered only when a tumor in motion enters a target area, using a real-time tumor-tracking radiotherapy (RTRT) system for patients with hepatocellular carcinoma who were untreatable with other modalities because the tumors were adjacent to crucial organs or located too deep beneath the skin surface.

Methods and Materials: Eighteen tumors, with a mean diameter of 36 mm, were studied in 15 patients. All tumors were treated on a hypofractionated schedule with a tight margin for setup and organ motion using a 2.0-mm fiducial marker in the liver and the RTRT system. The most commonly used dose of radiotherapy was 48 Gy in 8 fractions. Sixteen lesions were treated with a BED_{10} of 60 Gy or more (median, 76.8 Gy).

Results: With a mean follow-up period of 20 months (range, 3–57 months), the overall survival rate was 39% at 2 years after RTRT. The 2-year local control rate was 83% for initial RTRT but was 92% after allowance for reirradiation using RTRT, with a Grade 3 transient gastric ulcer in 1 patient and Grade 3 transient increases of aspartate amino transaminase in 2 patients.

Conclusions: Intercepting radiotherapy using RTRT provided effective focal high doses to liver tumors. Because the fiducial markers for RTRT need not be implanted into the tumor itself, RTRT can be applied to hepatocellular carcinoma in patients who are not candidates for other surgical or nonsurgical treatments. © 2007 Elsevier Inc.

Radiotherapy, Liver, Hepatocellular carcinoma, Real-time tumor-tracking radiotherapy.

INTRODUCTION

There are a number of nonsurgical local treatment techniques for the ablation of hepatocellular carcinoma (HCC), including radiofrequency ablation (RFA), percutaneous ethanol injection (PEI), and cryosurgery (1). These techniques require direct insertion of a needle or probe into the tumor mass. However, with HCC at deep locations, such as the top of the dome, near the inferior vena cava, or near the main portal vein, a needle or probe often cannot be inserted at the proper position. Transarterial embolization (TAE) is applicable only when one can identify the feeding artery, which is often difficult (2).

Radiotherapy has been a palliative treatment for patients with unresectable advanced HCC, but conventional radiotherapy is limited by the liver's low tolerance to large volumes of irradiation (3). Both focal radiotherapy using narrow-beam X-ray and particle therapy are expected to be useful for reducing radiation-induced liver damage (RILD) (4). When the tumor is close to the gastrointestinal (GI) tract, radiation-induced GI ulcer is a dreadful complication (5). Moreover, it is hard to increase the dose to the HCC when the tumor is in that position, owing to the large respiratory movement of the liver. In particle therapy, such as proton and carbon ion treatment, respiratory gating systems have been used to reduce the volume of normal tissue in the irradiated volume. As a result, the dose to the GI tract might be reduced in the particle therapy (6, 7).

In 1999 we began using a real-time tumor-tracking radiotherapy (RTRT) system to increase the accuracy of the nonsurgical treatment of tumors in motion (8). This has made intercepting radiotherapy possible for tumors in motion, whereby the tumor is irradiated only when it enters a target area, with a certain amount of permitted dislocation. After developing a technique to percutaneously insert a 2.0-mm gold

Reprint requests to: Hiroshi Taguchi, M.D., Department of Radiology, Hokkaido University Hospital, North-15 West-7, Sapporo 060-8638, Japan. Tel: (+81) 11-706-5975; Fax: (+81) 11-706-7876; E-mail: thiroshi@radi.med.hokudai.ac.jp

Supported by Grants-in-Aid from the Ministry of Education, Culture, Sports, and Technology in Japan (No. 18209039, No. 17016002).

Conflict of interest: none.

Received Oct 30, 2006, and in revised form Feb 27, 2007. Accepted for publication March 2, 2007.

fiducial marker into the liver and to confirm its localization stability (9), we suggested that intercepting radiotherapy using RTRT can be a radical radiotherapy for primary HCC (10). Because the fiducial marker does not need to be inserted directly into the tumor when RTRT is used, this method is applicable to more patients than is the case with percutaneous focal ablation techniques, such as RFA and cryosurgery. However, we have restricted the indication of RTRT to patients who were not eligible for other nonsurgical treatment techniques. In the present study, the outcomes of patients treated with the RTRT technique in the last 5 years were retrospectively analyzed to determine its proper indications for HCC.

METHODS AND MATERIALS

The focus of this study was on primary HCC diagnosed by dynamic computed tomography (CT) with the aid of serum tumor marker, according to the noninvasive Barcelona criteria (11). Patients were candidates if they were not eligible for any other treatment, such as surgery, RFA, PEI, and TAE. They were required to be 80 years old or younger and to have a Karnofsky performance status of 70% or more, as well as a liver function equivalent to Class A or B in the Child classification. Patients were excluded if they had uncontrolled ascites, obstructive jaundice, active gastroenteric bleeding, or a tendency to bleed. Patients who had tumor thrombosis of the portal vein or extrahepatic active metastatic disease on imaging examination were also excluded.

Multidetector CT was taken with a breath hold at the end of the expiratory phase of normal breathing. The slice thickness and interval were 2 mm. Gross tumor volume (GTV) was chosen to be compatible with the enhanced area in the early arterial phase of dynamic CT. Clinical target volume (CTV) was GTV plus a 5-mm margin three-dimensionally; thus the CTV diameter was 10 mm larger than the GTV. Planning target volume (PTV) was CTV plus a 5-mm margin three-dimensionally in principle. Modification of the PTV margin from 5 to 10 mm was allowed for the craniocaudal direction when no critical organs, such as the duodenum, were close to the edge of the PTV.

Dose–volume constraints were made for liver, lung, and GI tract according to previous reports and to our own preliminary studies. The maximum tolerable dose (MTD) to the liver adopted in this study was 30 Gy, using a 2-Gy daily dose for total liver volume (12). The biologic effective dose with an α/β ratio of 2 (BED_2) of the MTD was 60 Gy. The volume of liver that could receive 40 Gy in 20 fractions was assumed to be 30% of the whole liver in a dose–volume histogram. Alteration of dose fractionation was allowed to reduce the daily dose to the GI tract. The MTD of the GI tract was 40 Gy in 20 fractions, or BED_2 of 80 Gy. Based on these considerations, the total doses and fractionation schedules are listed in the study protocol as guidelines (Table 1). For example, if the tumor is >5 cm and the edge of the organ at risks is less than 1 cm, only 48 Gy in 8 fractions can be used. If the tumor is less than 3 cm and the edge of the GTV is 3 cm or more distant from the organ at risks, 20 Gy in one session or some other schedule can be used. This schema was developed to allow clinical staff members to select schedules based on the preliminary results of dose–volume statistics. Because of the insufficient data on the MTD, several dose schedules were allowed to be chosen.

Megavoltage X-rays (6, 10 MV) from a linear accelerator with five to seven single isocenter, non-coplanar ports were used. The dose was prescribed at the isocenter, giving 80% of the isocentric dose to cover PTV. A round, 2-mm gold marker was implanted near the tumor, within 3 cm from the isocenter of the GTV in principle. The reliability of the inserted marker as the GTV surrogate has already been reported (9). In short, the relationship between the gravity center of the liver and the marker was reproducible in the sequential CT examination for more than 1 month. Two sets of fluoroscopic cameras in the treatment room were used for the real-time recognition of the marker every 0.033 s during the delivery of the therapeutic beam. The therapeutic beam was gated to irradiate the tumor only when the marker was within 2.0 mm of the planned coordinates in lateral, anteroposterior, and craniocaudal directions.

The patients were followed up with a physical examination, blood collection, and either CT or magnetic resonance imaging every 3 months for 1 year and every 4–6 months thereafter by radiation oncologists with the help of hepatologists.

The Kaplan-Meier method was used to calculate the overall survival, local control, and intrahepatic control rates, in which any new lesions were counted as a failure. Adverse effects were scored according to National Cancer Institute Common Toxicity Criteria for Adverse Events, version 3.

RESULTS

From 2001 to 2004, 18 lesions of 15 patients were entered into this study. The patients were aged 54–73 years (median, 57 years). Hepatic function before radiotherapy was classified as Child class A, B, and C in 12, 3, and 0 patients, respectively. Five patients suffered from hepatitis B virus, 9 from hepatitis C virus, and 1 from alcoholic hepatitis. Tumors were located at the hepatic segments S1, S2, S6, S7, and S8 according to the Couinaud classification (13) in 3, 4, 3, 1, and 7 patients, respectively. The tumor diameter ranged from 15 to 52 mm (mean, 36 mm; standard deviation, 14 mm).

The reasons for RTRT were as follows: too close to the portal vein or inferior vena cava for other treatments, such as RFA or PEI, in 4 patients; located at the hepatic dome (S8) and far from other treatments in 3 patients; residual disease after other treatment in 2 patients; and coexisting illness in 3 patients.

The prescribed doses and fractionation used in the actual study are shown in Table 1. Various schedules were used according to the size and position of the tumor to restrict the dose to the critical organ. The most common dose in this study was 48 Gy in 8 fractions. The biologic effective dose with an α/β ratio of 10 (BED_{10}) was distributed from 39 to 106 Gy without consideration for cell proliferation. Seventeen lesions were treated with a BED_{10} of $\geq$50 Gy, and 16 lesions were treated with a BED_{10} of $\geq$60 Gy or more (median, 76.8 Gy).

With a mean follow-up period of 20 months (range, 3–57 months), the overall survival rate was 44% (standard error [SE] 14%) at 21 months after RTRT (Fig. 1). Rates of 1- and 2-year actuarial survival after RTRT were 79% and 44%, respectively. The local control rate within the CTV was 83% (SE 11%) at 30 months after RTRT. The intrahepatic control rate was 34% (SE 13%) at 10 months and 17% at 2 years after RTRT (Fig. 1). There were two local failures. One patient with a 20-mm tumor was treated with 48 Gy in 8 fractions in 2 weeks and relapsed at 8 months from the

Table 1. Doses and fractionations used in the intercepting radiotherapy

			Tumor size (GTV) (cm)			Distance from OAR (cm)†		
Dose (Gy)/fraction	*n*	BED_2/BED_{10} (Gy)*	<3	3–5	>5	<1	1–3	>3
20/1	1	220/60	1	—	—	—	—	1
48/4	1	336/106	—	1	—	—	—	1
40/4	3	240/80	1	1	1	—	1	2
48/8	7	192/76.8	1	5	1	1	4	2
40/8	2	140/60	—	2	—	—	2	—
40/16	1	90/50	—	1	—	—	1	—
Out of protocol	3	37/8, 30/10, 40/20+36/8	—	2	1	2	1	—

Abbreviations: GTV = gross tumor volume; OAR = organ at risk.
Tumor sizes and distances from the organ at risk of the patients treated are shown for each dose/fractionation schedule.
* Biologic equivalent dose, assuming an α/β ratio of 2 and 10 for BED_2 and BED_{10}, respectively.
† Minimum distance between the edge of clinical target volume and OAR.

margin of the tumor. The patient was treated by TAE afterward and survived for 21 months. The other patient, with a 15-mm tumor, was treated with 20 Gy in one session and relapsed at 10 months from the inside of the GTV. The latter was treated again with RTRT, and the tumor was controlled for 8 months thereafter. No other patients received transarterial chemoembolization or local ablation in combination with RTRT. In cases in which we allowed reirradiation for the relapsed tumor as a part of the treatment, the local control rate of the radiotherapy was 92% at 30 months. The 2- and 5-year actuarial survival rates after the initial treatment for HCC were 93% and 52%, respectively.

A symptomatic complication due to the insertion of the fiducial marker occurred in 1 patient, who experienced transient bile ductal bleeding and inflammation. An adverse reaction due to radiation was seen in 2 patients. A transient gastric ulcer in a patient with a 50-mm tumor adjacent to the stomach was salvaged by emergency endoscopic treatment (Grade 3 adverse effect), and the patient has been alive with no evidence of disease at 58 months. Radiation pneumonitis in a patient with a 45-mm tumor at the hepatic dome without the requirement of medication (Grade 1 adverse effect) was observed at 4 months after RTRT. No radiologic change was found in the follow-up CT taken at 20 months after RTRT.

There were no encephalopathy and ascites in the patients without tumor progression. Changes in transaminase levels after RTRT were available in 10 patients and are shown in Fig. 2. Several patients experienced increased transaminase at the subacute phase after RTRT transiently. There was no Grade 4 toxicity of liver function due to radiation, and there were two Grade 3 toxicities of transient elevation of aspartate amino transaminase (elevation at least 5 to 10 times the upper limit of normal).

DISCUSSION

Localized X-ray radiotherapy has been shown to achieve excellent local control rates with lower rates of radiation-induced liver dysfunction compared with conventional radiotherapy (4). Park *et al.* (14) reported a dose–response relationship in the local control rate of primary HCC. More recently, Park *et al.* (15) reported achieving an objective tumor response in 39 of 59 patients (66.1%), with complete response

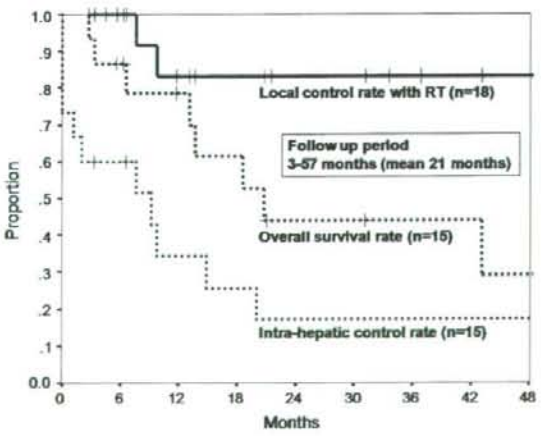

Fig. 1. Kaplan-Meier curves of overall survival and intrahepatic control rates for 15 patients with hepatocellular carcinoma (HCC) and local control rate with reirradiation for 18 HCC in the 15 patients. RT = radiotherapy.

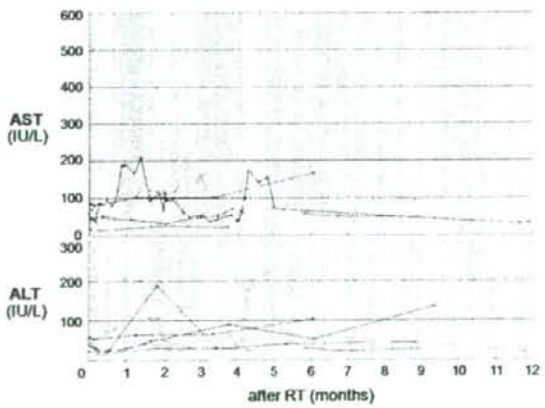

Fig. 2. Changes in transaminases. Alanine amino transaminase (ALT) and aspartate amino transaminase (AST) levels after real-time tumor-tracking radiotherapy (RT) in 10 patients.